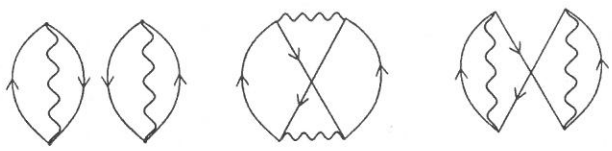

Figure 1.7.1: Oyster diagrams describing the correlation of the nuclear ground state associated with the ZPF of collective particle–hole–like excitations, and Pauli principle correction processes in which fermions are exchanged. This is in keeping with the fact that the collective modes are built out of the particle degrees of freedom (see e.g. Fig. 1.D.1).

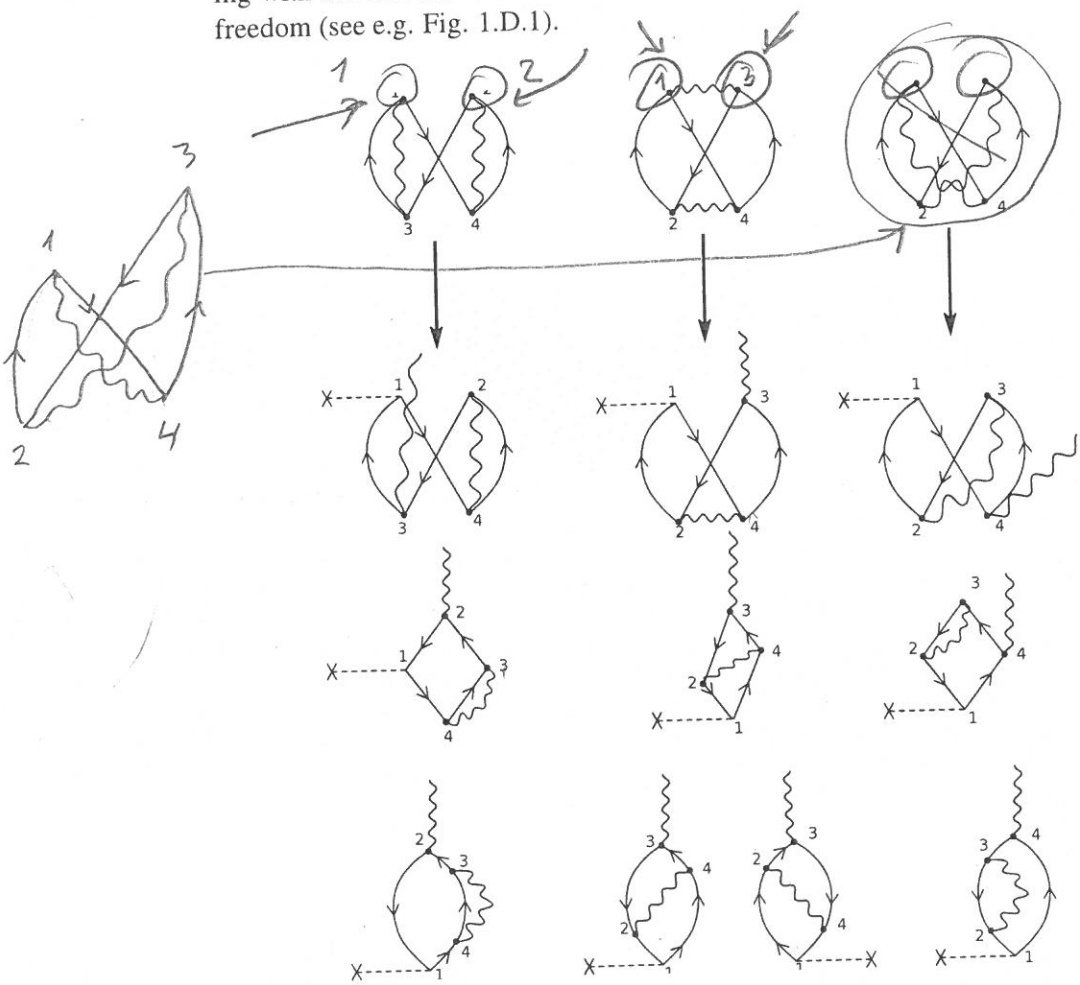

Figure 1.7.2: Some of the possible outcomes resulting from acting with a single–particle field, e.g. that associated with inelastic processes (represented by a horizontal dashed line starting with a ×), on the Pauli corrected ZPF oyster diagrams associated with collective $(p-h)$ excitations of the nuclear vacuum (see Fig. 1.7.1). Within this context one returns to the question of renormalization mentioned in the text (see end of Sect. 1.1 and Sect. 1.4, see also Idini et al. (2015), Broglia et al. (2016), Barranco et al. (2017a); see also Sect. 6.5).

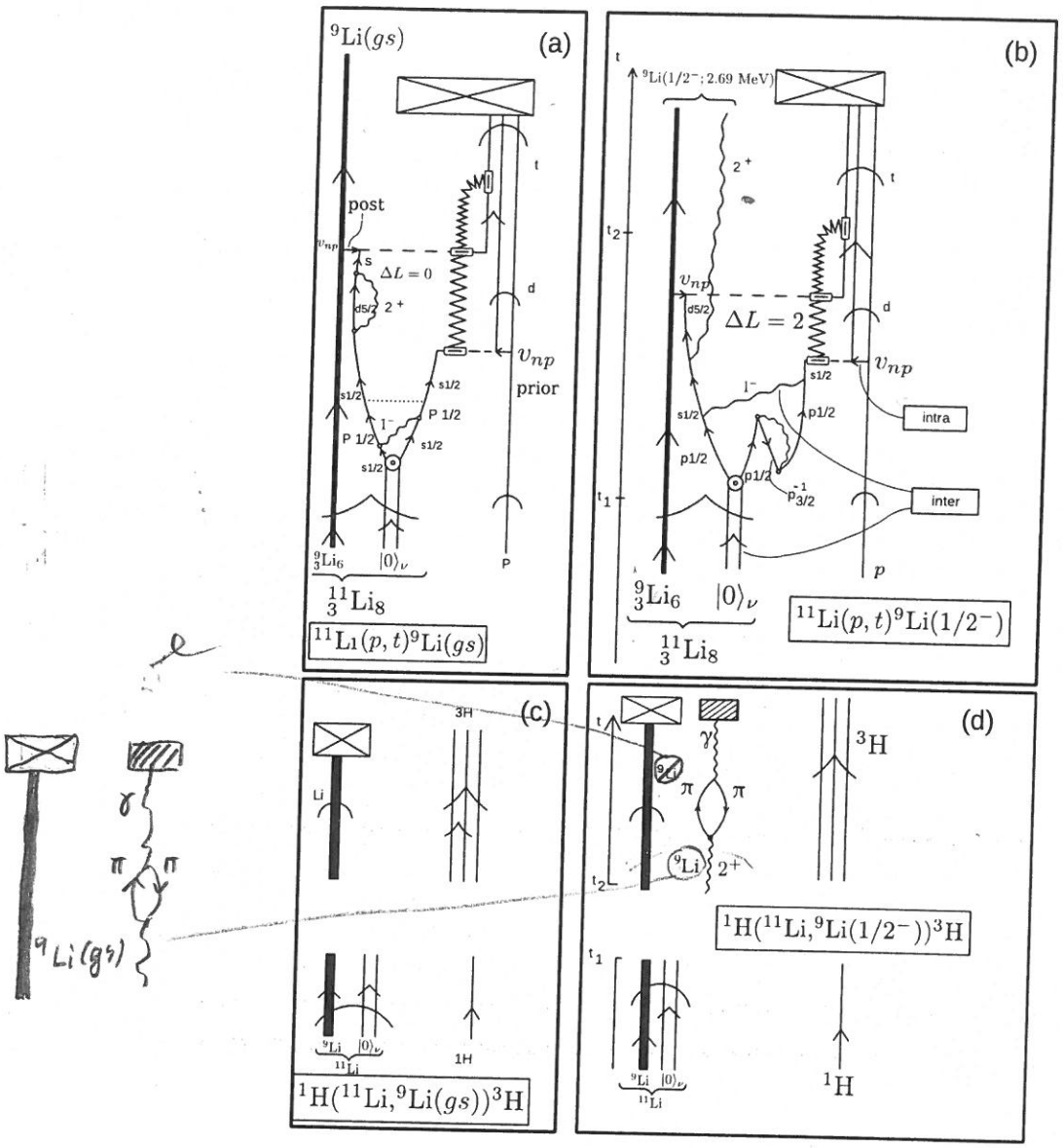

Figure 1.9.3: NFT representation of the reactions (a) ^{11}Li$(p,t)^9$Li(gs), (b) ^{11}Li$(p,t)^9$Li$(1/2^-)$, (c) ^{1}H$(^{11}$Li,^{9}Li(gs))^{3}H and (d) ^{1}H$(^{11}$Li,^{9}Li$(1/2^-))^3$H. Time is assumed to run upwards. A single arrowed line represents a fermion (proton) (p) or neutron (n). A double arrowed line two correlated nucleons. In the present case two correlated (halo) neutrons (halo-neutron pair addition mode $|0>_\nu$). A heavy arrowed line represents the core system $|^9$Li(gs)>. A standard pointed arrow refers to structure, while "round" arrows refer to reaction. A wavy line represents (particle-hole) collective vibrations, like the low-lying quadrupole mode of ^{9}Li, or the dipole pygmy resonant state which, together with the bare pairing interaction (horizontal dotted line) binds the neutron halo Cooper pair to the core. A short horizontal arrow labels the proton–neutron interaction v_{np} responsible for the single–particle transfer processes, represented by an horizontal dashed line . A dashed open square indicates the particle-recoil coupling vertex. The jagged line represents the recoil normal mode resulting from the mismatch between the relative centre of mass coordinates associated with the mass partitions ^{11}Li+p, ^{10}Li+d (virtual) and ^{9}Li+t. The γ–detector is represented by a hatched box (see Fig. 6.6.2), the particle detector by a crossed rectangle. For further details see caption Fig. 1.9.2.

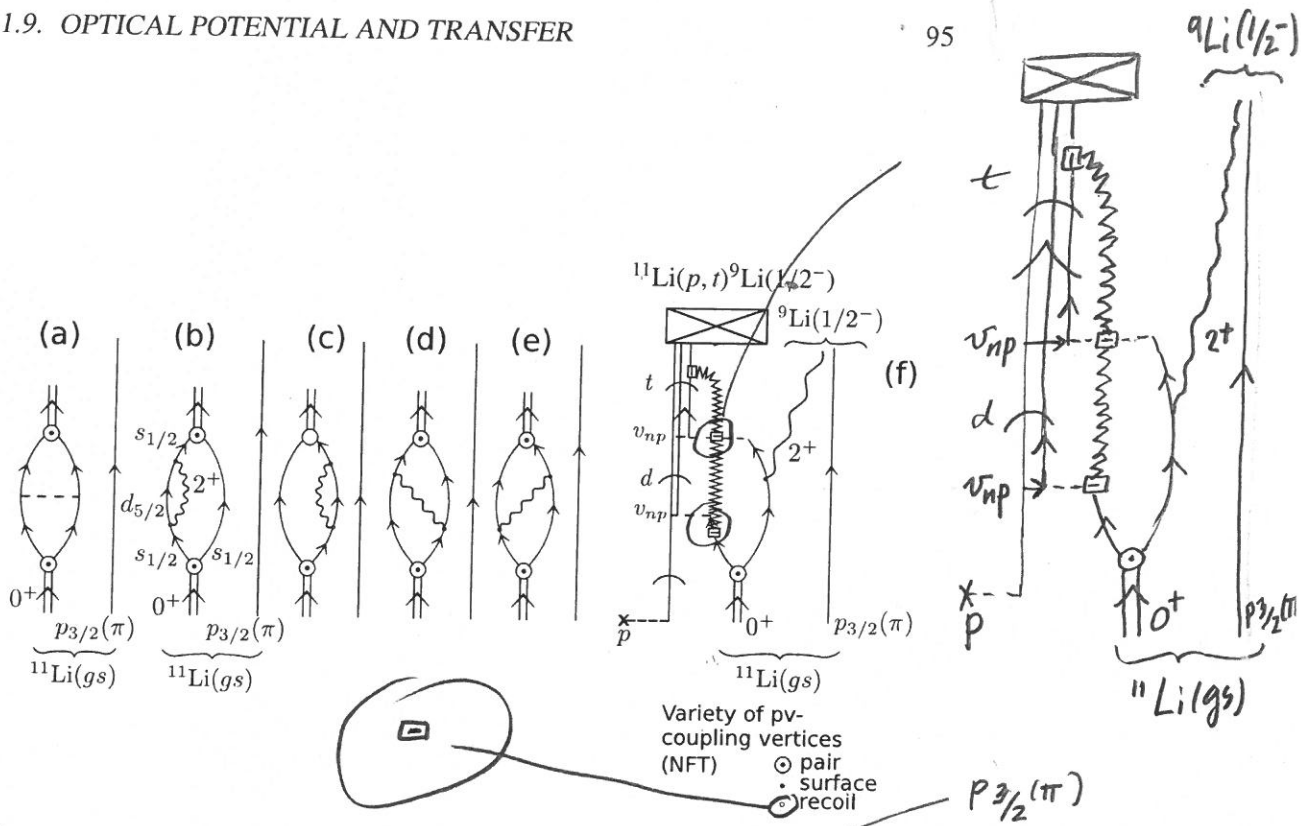

Figure 1.9.4: (**a–e**) Lowest order, NFT diagrams associated with the processes contributing to the binding of the neutron halo Cooper pair (double arrowed line) of ^{11}Li to the core ^{9}Li through the bare pairing interaction (dashed line) as well as the exchange of the core quadrupole phonon and of the soft dipole mode of ^{11}Li (wavy line). Single arrowed lines describe the nucleon independent–particle motion of neutrons ($s_{1/2}, d_{5/2}$, etc.) as well as of the proton considered as a spectator; (**a**) Bare pairing interaction, four–point vertex (horizontal dashed line); (**b, c**) self energy, effective mass polarization (PO) process dressing the $s_{1/2}(\nu)$ single–particle state (a similar diagram, but corresponding to correlation (CO) processes (see Fig. 4.2.4) dressing the $p_{1/2}$ state are not shown, see Figs. 1.9.2 and 1.9.3); (**d, e**) vertex correction (induced interaction) renormalizing the vertex with which the pair addition mode couples to the fermion (dotted open circle); (**f**) NFT diagram describing the reaction ^{11}Li$(p,t)^{9}$Li$(1/2^-)$ populating the first excited state of ^{9}Li, the dashed horizontal line starting with a cross standing for the (p,t) probe. The successive transfer of the two halo neutrons (^{11}Li(gs)$+p \rightarrow{}^{10}$Li$+d \rightarrow{}^{9}$Li$(1/2^+)+t$) is shown, in keeping with the fact that this process provides the largest contribution to the absolute differential cross section. The jagged line represents the recoil mode carrying to the outgoing nucleus the effect of the momentum mismatch associated with the transfer process (recoil).

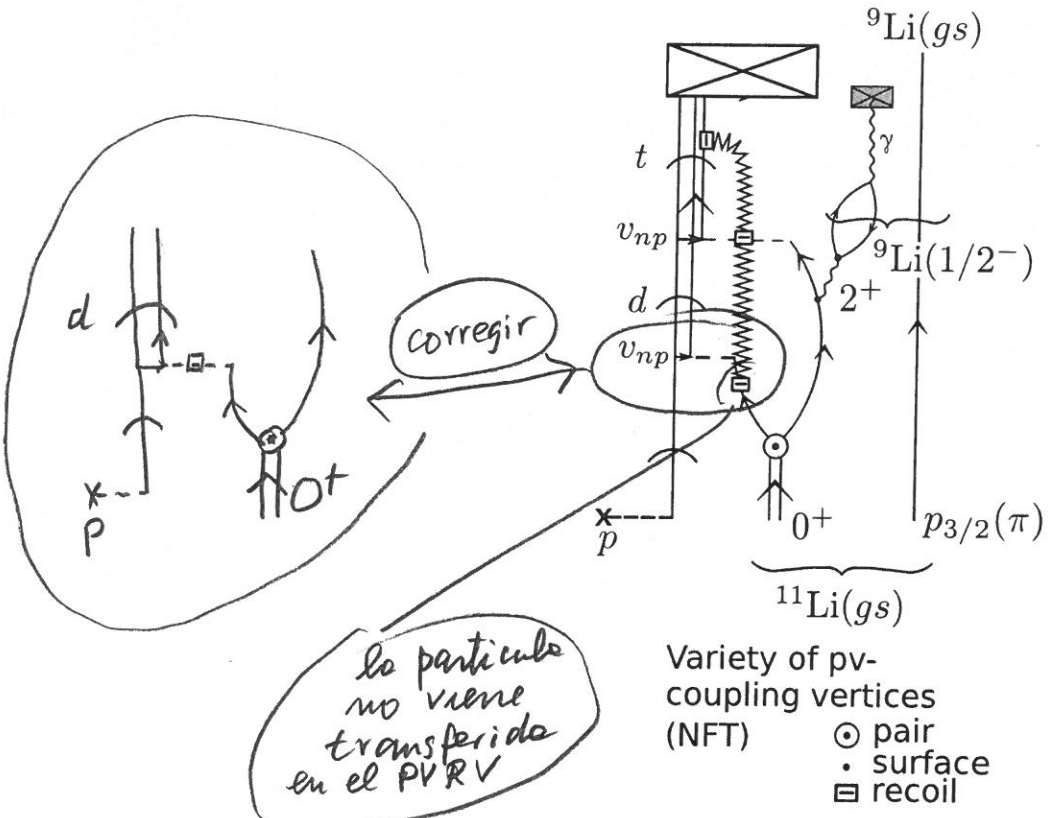

Figure 1.9.5: Gedanken γ–ray coincidence experiment ^{1}H(^{11}Li,^{9}Li)^{3}H and ^{9}Li(gs)+γ($E2$; 2.69 MeV). In this case, the virtual quadrupole phonon associated with self–energy and vertex correction processes becomes real through the action of the (p, t) external field. Thus, it is not only that recoil modes are "measured" by detectors in connection with outgoing particles which have asymptotic wavefunctions, but also the quadrupole vibration, whose eventual γ–decay (see Fig. 6.6.2 (II)) can be measured by the γ–detector.

Fig. 1.9.6 te da un ejemplo correcto

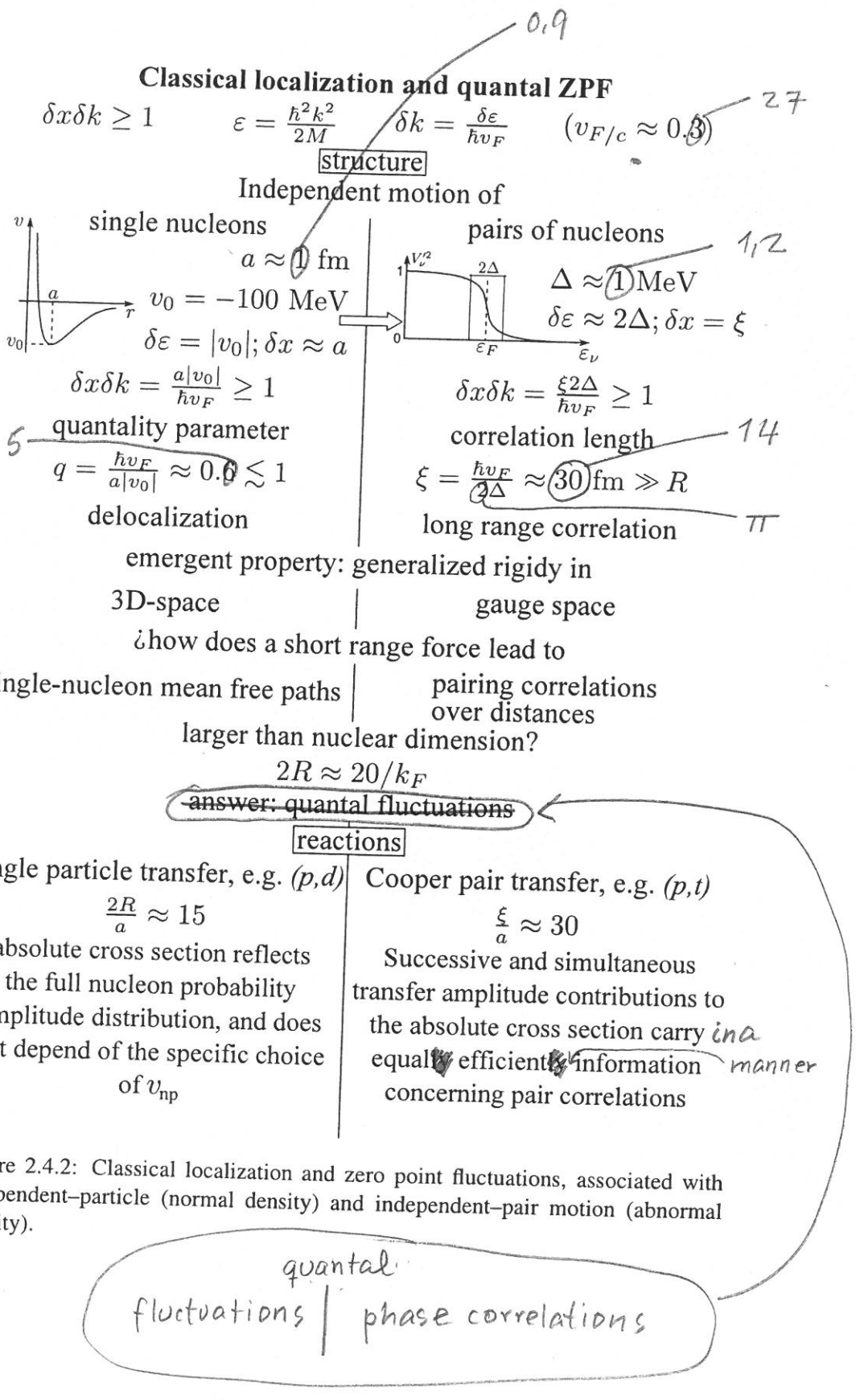

Figure 2.4.2: Classical localization and zero point fluctuations, associated with independent–particle (normal density) and independent–pair motion (abnormal density).

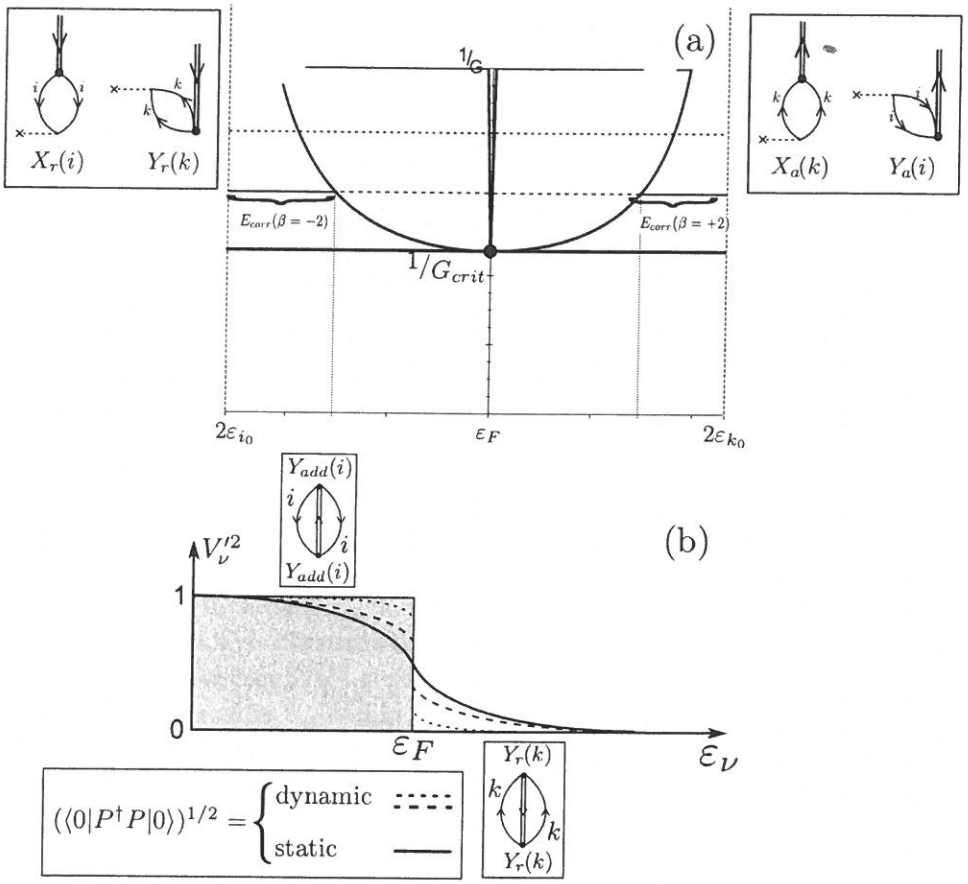

Figure 2.5.6: Schematic representation of the quantal phase transition taking place as a function of the pairing coupling constant in a (model) closed shell nucleus. (a) dispersion relation associated with the RPA diagonalization of the Hamiltonian $H = H_{sp} + H_p$ for the pair addition and pair removal modes. In the insets are shown the two-particle transfer processes exciting these modes, which testify to the fact that the associated zero point fluctuations (ZPF) which diverge at $G = G_{crit}$, blur the distinction between occupied and empty states typical of closed shell nuclei. (b) occupation number associated with the single-particle levels. For $G < G_{crit}$ there is a dynamical depopulation (population) of levels $i(k)$ below (above) the Fermi energy. For $G > G_{crit}$, the deformation of the Fermi surface becomes static, although with a non–vanishing dynamic component (cf. Fig. 2.1.2).